

Available online at [www.sciencedirect.com](http://www.sciencedirect.com)

SciVerse ScienceDirect

Energy Procedia 22 (2012) 119 – 126

Energy  
Procedia

E-MRS 2011 Spring Meeting Symposium T

TaO<sub>x</sub>N<sub>y</sub> sputtered photoanodes for solar water splittingC.M. Leroy<sup>a\*</sup>, R. Sanjines<sup>b</sup>, K. Sivula<sup>a</sup>, M. Cornuz<sup>a</sup>, N. Xanthopoulos<sup>c</sup>, V. Laporte<sup>c</sup>, M. Grätzel<sup>a</sup><sup>a</sup>Laboratory of Photonics and Interfaces (LPI), Ecole Polytechnique Fédérale de Lausanne (EPFL), 1015 Lausanne, Switzerland<sup>b</sup>Institute of Condensed Matter Physics, Ecole Polytechnique Fédérale de Lausanne (EPFL), 1015 Lausanne, Switzerland<sup>c</sup>Interdisciplinary Centre for Electron Microscopy (CIME), Ecole Polytechnique Fédérale de Lausanne (EPFL), 1015 Lausanne, Switzerland**Abstract**

A series of TaO<sub>x</sub>N<sub>y</sub> photoelectrodes were deposited on F:SnO<sub>2</sub> (FTO) substrates by DC reactive sputtering at room temperature, under a mixture of Ar, N<sub>2</sub> and O<sub>2</sub>. The effects of the O<sub>2</sub> partial pressure during deposition (P<sub>O2</sub>) on the films crystallinity, their chemical composition, their morphology as well as their absorption and photoelectrochemical properties have been investigated. The increase of P<sub>O2</sub> led to the modification of film crystallinity, which evolved from a semicrystalline Ta<sub>3</sub>N<sub>5</sub> structure to an amorphous state. The increase of the P<sub>O2</sub> also led to the increases of the oxygen content, of the bandgap energy and of the films roughness. Preliminary photoelectrochemical (PEC) investigations have been performed through current-voltage measurements. An optimal P<sub>O2</sub> has been highlighted, corresponding to a tradeoff between, on the one hand, the amorphization of the films – which degrades PEC performances – and on the other, the tuning of the chemical composition as well as of the bandgap energy.

© 2012 Published by Elsevier Ltd. Selection and/or peer review under responsibility of European Material Research Society (E-MRS)  
Open access under [CC BY-NC-ND license](https://creativecommons.org/licenses/by-nc-nd/4.0/).

Keywords: tantalum; oxynitrides; nitrides; sputtering; water splitting

**1. Introduction**

In the context of an increasing clean energy demand, solar water splitting has become the object of extensive research as this is one of the most promising routes to produce and store sustainable energy in the form of hydrogen. Materials used for such an application must fulfill several requirements among which are suitable band gap and band edge positions while demonstrating good stability, good charge transport properties, good kinetics, low toxicity and reduced cost [1].

Many oxides are excluded because their band gap is too large. Nitrogen 2p orbitals stand at higher energy than oxygen 2p orbitals, which usually contribute to the top of the valence band in oxides. The substitution of oxygen by

\* Corresponding author. Tel.: +41-216-933-624; fax: +41-216-934-111.

E-mail address: [celine.leroy@epfl.ch](mailto:celine.leroy@epfl.ch)

nitrogen leads to the elevation of the top of the valence band and therefore to the decrease of the band gap. Thus, the band gap of an oxynitride can be easily tuned by simply adjusting the nitrogen content [2, 3].

Among the existing (oxy)nitrides,  $\beta$ -TaON and  $\text{Ta}_3\text{N}_5$  are promising candidates as photoanode materials for solar water splitting. Their interest results from (i) their abilities to absorb visible light up to ca. 530 nm (2.34 eV) and 600 nm (2.1 eV), respectively; as well as from (ii) their valence band maximum and conduction band minimum that lie, for TaON, at ca. +2.2 V vs. NHE and -0.3 V vs. NHE at pH 0, respectively; and for  $\text{Ta}_3\text{N}_5$ , at ca. +1.6 V vs. NHE and -0.4 V vs. NHE at pH 0, respectively.[4] This implies that – contrary to state-of-the-art photoanode materials such as  $\text{Fe}_2\text{O}_3$  or  $\text{WO}_3$  whose conduction bands are located below the water reduction potential – these materials can potentially split water without any external bias.

In the past, TaON photoelectrodes prepared by electrophoretic deposition of TaON powder and  $\text{Ta}_3\text{N}_5$  photoelectrodes prepared by nitridation of surface-oxidized Ta sheets have demonstrated good performances [5, 6]. However, the synthesis methods employed do not allow to precisely control properties such as the thickness or the composition of the photoelectrodes. Recently, these limitations have been circumvented with  $\text{Ta}_3\text{N}_5$  photoanodes prepared on Ta or Ti substrates by RF reactive sputtering at 897-1113K, followed by a post-treatment under  $\text{NH}_3$  [7]. These photoanodes also demonstrated promising performance but the effects of the deposition conditions on the PEC performances were not investigated. More generally, whatever the aforementioned preparation method, it always involved thermal treatments under  $\text{NH}_3$ , which can be fastidious, risky and detrimental for conductive substrates.

In this study,  $\text{TaO}_x\text{N}_y$  photoanodes were deposited by DC reactive sputtering at room temperature and without any use of  $\text{NH}_3$ . The effects of the deposition conditions on the photoanodes chemical and physical properties have been investigated. In particular, preliminary results on their PEC performances will be presented.

## 2. Experimental

$\text{TaO}_x\text{N}_y$  films were deposited on 12 mm x 30 mm FTO substrates (F:SnO<sub>2</sub> on float glass TEC 15, Hartford Glass Co.) by DC reactive sputtering at room temperature and in a mixture of Ar, N<sub>2</sub> and O<sub>2</sub>. The total pressure was about  $7.5 \times 10^{-3}$  mbar. A 5 cm-diameter Ta target (99.95%, Kurt J. Lesker Co.) was used with a distance to the substrate of 9 cm. Prior to the deposition, the target was pre-sputtered in Ar for 5 min., then in the Ar/N<sub>2</sub>/O<sub>2</sub> mixture for another 5 min. The DC current was maintained at 250 mA during the pre-sputtering and the deposition. Deposition was performed for 25 min. leading to 90 nm-thick  $\text{TaO}_x\text{N}_y$  films, the thickness having been measured with a TENCOR Alpha-Step 500 profilometer.

The films composition was assessed by Auger Electron Spectroscopy (AES). Analyses were performed with a Perkin-Elmer PHI 660 Scanning Auger Microprobe in the Surface Analysis Facility of the Interdisciplinary Centre for Electron Microscopy at EPFL. Primary electron beam potential and current were 5 kV and 10 nA, respectively. Depth profiling was performed to check the stability of the sputtered films' composition throughout all the thickness. It was made using 2 keV argon ions and the sputtering rate was  $4.5 \text{ nm} \cdot \text{min}^{-1}$  as calibrated with 100 nm Ta<sub>2</sub>O<sub>5</sub>/Ta NPL standard.

The film surface morphology was characterized by High Resolution Scanning Electron Microscopy (HRSEM) and Atomic Force Microscopy (AFM). The tilted cross-sections of the  $\text{TaO}_x\text{N}_y$  films deposited on FTO substrates were investigated with a high-resolution scanning electron microscope equipped with a field emission gun (Philips XL-SFEG). The images were taken with an acceleration voltage of 3 keV and a 3 mm working distance using an in-lens detector. AFM was performed using a TMX 2000 Explorer SPM, Topometrix (USA) apparatus in no contact mode. The crystallinity was investigated by grazing incidence X-Ray Diffraction (XRD) at an angle of 6° with a Bruker D8 Advance diffractometer operating in Bragg-Brentano geometry. The transmission spectra have been recorded between 200 and 800 nm on a CARY 5000 UV-VIS-NIR spectrophotometer and for films sputtered on quartz.

Photocurrent measurements were performed under front-side chopped irradiation and in a three-electrode configuration using a 0.1 M Na<sub>2</sub>SO<sub>4</sub> aqueous solution (pH 7) as the electrolyte, a Pt wire as the counter electrode, and an Ag/AgCl electrode in saturated KCl solution as the reference electrode. The light source was simulated

sunlight from a 450 W xenon lamp (Osram, ozone free) passed through a KG3 filter (3 mm, Schott) with a measured intensity equivalent to standard AM1.5 sunlight ( $100 \text{ mW.cm}^{-2}$ , spectrally corrected).

### 3. Results and discussion

The photoelectrochemical properties of materials are strongly dependant on (i) their crystallinity, the defects of which can act as recombination centers; (ii) their morphological properties such as their surface area or the feature size that charge carriers have to travel through; (iii) their absorption properties which must be optimal with regard to light harvesting; and (iv) their composition which will govern the material surface's reactivity but will also have an influence on the other properties. Therefore, correlations between the  $\text{O}_2$  partial pressure during deposition ( $P_{\text{O}_2}$ ) and the properties aforementioned have first been investigated in order to determine the optimal synthesis conditions and identify any limiting factors that should be overcome in the future.

The most trivial correlation between the  $P_{\text{O}_2}$  and the sputtered films properties that can be expected concerns the film composition. Table 1 shows the evolution of the chemical composition as a function of the  $P_{\text{O}_2}$ . The atomic percentages measured throughout the whole  $\text{TaO}_x\text{N}_y$  film thickness during the depth profiling were averaged and allowed for the calculation of ratios reported in table 1. It appeared that the  $\text{N}/(\text{N}+\text{O})$  ratio decreased from 86% to 28% when the  $P_{\text{O}_2}$  was increased from 0 to  $4.2 \times 10^{-4}$  mbar. This confirmed that – logically – the oxygen content could be easily controlled through the  $P_{\text{O}_2}$ .

Table 1: Chemical composition ratios of the  $\text{TaO}_x\text{N}_y$  sputtered photoanodes as a function of the  $P_{\text{O}_2}$  and determined by AES analysis.

$P_{\text{O}_2}$ ( $10^{-4}$ .mbar)	Ta/(Ta+N+O) ratio (%)	N/(Ta+N+O) ratio (%)	O/(Ta+N+O) ratio (%)	N/(N+O) ratio (%)
0	48	45	7	86
0.9	44	47	8	85
1.9	41	41	17	70
3	37	31	32	49
4.2	34	19	47	28

To examine the  $X/(\text{Ta}+\text{N}+\text{O})$  ratios, where  $X=\text{Ta}$ ,  $\text{N}$  or  $\text{O}$ , it has to be mentioned that the evaluation of the content of light elements such as nitrogen and oxygen by means of AES often results in underestimated values [8]. Therefore, the trends observed regarding to the  $X/(\text{Ta}+\text{N}+\text{O})$  ratios have to be considered with caution. It was clear that as the  $P_{\text{O}_2}$  was risen, the  $\text{Ta}/(\text{Ta}+\text{N}+\text{O})$  ratio decreased. At low  $P_{\text{O}_2}$ , this ratio seemed closer to the one encountered in  $\text{TaN}$  phases but, taking into the potential underestimation of the nitrogen content, this ratio could also be compatible with other tantalum nitrides such as  $\text{Ta}_3\text{N}_5$ ,  $\text{Ta}_4\text{N}_5$  or even  $\text{Ta}_5\text{N}_6$ . At high  $P_{\text{O}_2}$ , the  $X/(\text{Ta}+\text{N}+\text{O})$  ratios became closer to the ones encountered in the  $\text{TaON}$  phase.

Beside the chemical composition, the crystallinity and the morphological properties of the films have been investigated by XRD, SEM and AFM.

Figure 1 illustrates the evolution of the XRD patterns as a function of the  $P_{\text{O}_2}$ . Below  $0.9 \times 10^{-4}$  mbar, the diffractograms exhibited reflections that could be assigned to the  $\text{Ta}_3\text{N}_5$  phase (JCPDS 01-072-0813), which was consistent with the AES results. Only a few broad peaks could be observed which indicates that the films were poorly crystallized. Beyond a  $P_{\text{O}_2}$  of  $0.9 \times 10^{-4}$  mbar, the films became amorphous.

Such an amorphization of sputtered layers, going from oxides or nitrides phases toward their oxynitrides counterparts through the adjustment of the  $P_{\text{O}_2}$  or the  $P_{\text{N}_2}$ , is well known and has already been reported for  $\text{TiO}_x\text{N}_y$ ,  $\text{HfO}_x\text{N}_y$  or  $\text{ZnO}_x\text{N}_y$  films [9, 10]. This behavior might have two concomitant origins: on the one hand, the defect creation due to the anionic substitution which destabilizes the lattice and leads to a crystallization delay; and on the other, the competition between the formation of the different phases involved, which in our case would be the  $\text{Ta}_3\text{N}_5$ , the  $\text{TaON}$  and the  $\text{Ta}_2\text{O}_5$  phases. This last assumption is reinforced by the AES trends which showed that –

although the chemical composition does not guaranty the phase(s) that will nucleate - the elemental ratios could be compatible with more of one of these phases depending on the  $P_{O_2}$ .

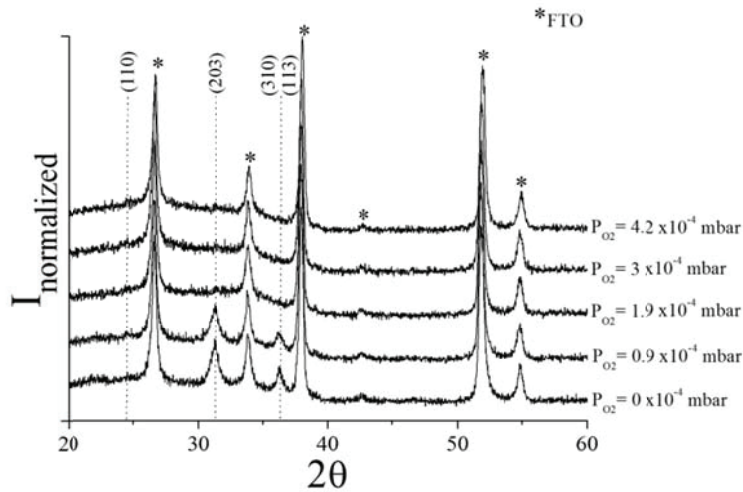


Figure 1: XRD patterns of the  $TaO_xN_y$  films as function of the  $P_{O_2}$ . The reported reflections correspond to the  $Ta_3N_5$  phase. The intensities have been normalized with regard to the most intense reflection of the FTO substrates.

Figures 2a and 2c show the SEM tilted cross sections of the films deposited without oxygen and with a  $P_{O_2}$  of  $1.9 \times 10^{-4}$  mbar, respectively. The thicknesses of the  $TaO_xN_y$  layers were consistent with the profilometer measurements which suggested a constant thickness of ca. 90 nm regardless of the  $P_{O_2}$ . The SEM micrographs also highlighted smoother surfaces as the  $P_{O_2}$  was increased.

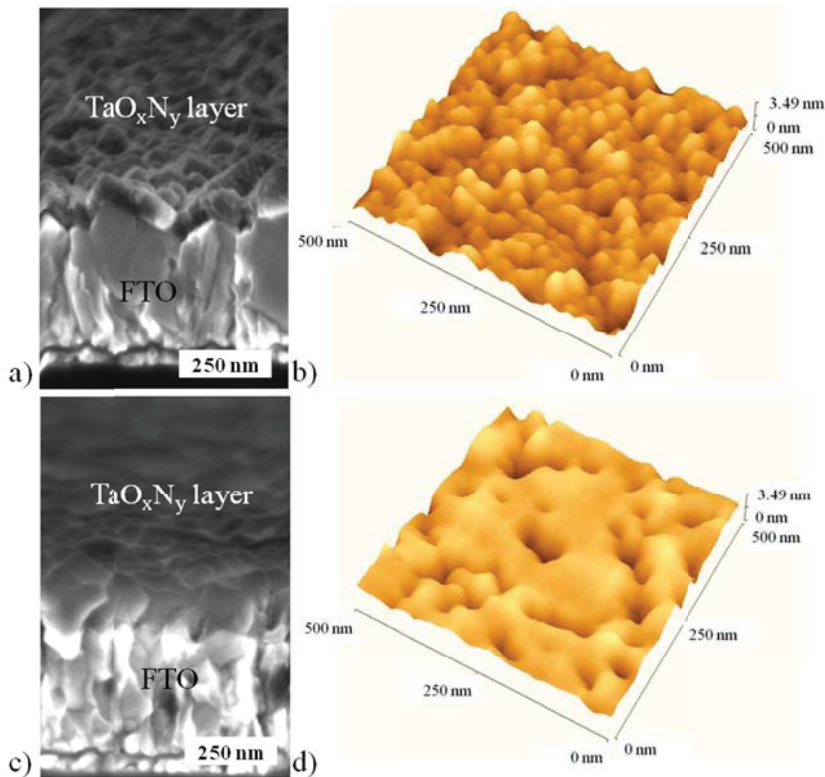


Figure 2: a,c) HRSEM micrographies of the tilted cross-sections and b,d) AFM images of the  $TaO_xN_y$  films deposited on FTO a,b) without oxygen or c,d) with a  $P_{O_2}$  of  $1.9 \times 10^{-4}$  mbar.

The morphological investigations have been completed with AFM studies (Figures 2b and 2d), which revealed root-mean-square (rms) roughnesses of 0.5 and 1.9 nm for the films deposited without oxygen or with a  $P_{O_2}$  of  $1.9 \times 10^{-4}$  mbar, respectively. As the roughness of films generally increases with their thickness, the later property has to be constant in order to study the influence of any parameter on the roughness. As this was the case here, this allowed us to safely conclude from the AFM measurements that the roughness was increasing with the  $P_{O_2}$ .

The morphological trends revealed by the SEM and AFM investigations could be correlated with the films crystallinity. For low  $P_{O_2}$ , films were semi-crystalline. Thus, the crystallites growth explained the more granular and sharper surface features. As the  $P_{O_2}$  increased, the delay of the crystallites formation led to smoother surface features. However, despite this last trend that should exacerbate the roughness, the contrary was observed. This means that the increase of the  $P_{O_2}$  likely introduced some porosity which led to the increase of the roughness.

The motivation of nitrogen or oxygen incorporation within oxides or nitrides is to modify the bandgap of the starting material so that the resulting one exhibits optimal absorption properties with regard to the solar water splitting requirements. As the AES analysis demonstrated that the O/N ratio could be adjusted within the  $TaO_xN_y$  films through the control of the  $P_{O_2}$ , the absorption properties were expected to reflect this ratio's modification and then to be affected to some extent by the  $P_{O_2}$ .

Figure 3 represents the transmission spectra of the  $TaO_xN_y$  films sputtered on quartz. The increase of the  $P_{O_2}$  led to a shift of the absorption front toward shorter wavelengths. A similar shift, on the same wavelength range, was observed by Banakh *et al.* with  $TaO_xN_y$  films deposited at  $300^\circ\text{C}$  by pulsed reactive gas DC sputtering and which O/N ratios were in the same range [11]. Such a shift indicates that the film's bandgap energy was increased. This confirms that – due to its direct influence on the O/N ratio – the control of the  $P_{O_2}$  is a means to tune the bandgap energy of sputtered oxynitrides films.

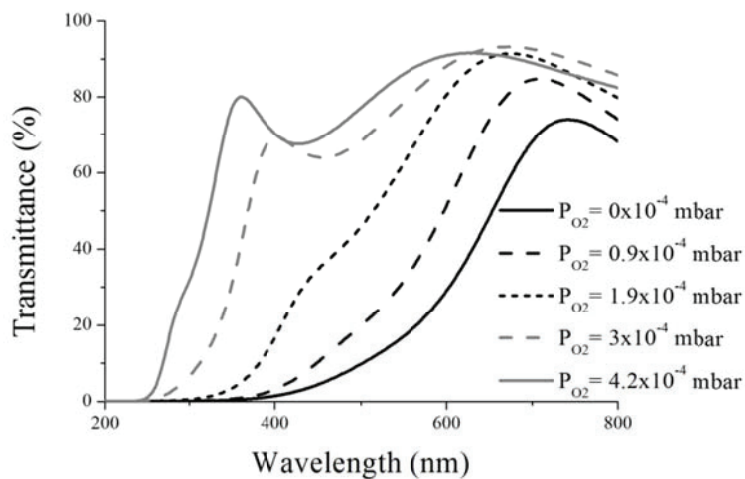


Figure 3: Transmission spectra of the  $TaO_xN_y$  sputtered films deposited at different  $P_{O_2}$  on quartz.

As the  $P_{O_2}$  strongly affected some of the  $TaO_xN_y$  films properties that are able to influence the PEC performance, *i.e.* their chemical composition, their crystallinity, their morphology and their bandgap energy, the relation between the  $P_{O_2}$  and the PEC properties has been studied. Current-voltage measurements have been performed as preliminary investigations in order to determine the optimal synthesis conditions. The measurements were performed under AM1.5 illumination, in an aqueous solution containing 0.1M of  $Na_2SO_4$ . All samples generated anodic photocurrents except for the  $P_{O_2}$  extrema, *i.e.* at 0 mbar and  $4.2 \times 10^{-4}$  mbar.

Figure 4a shows the evolution of the photocurrent density at 1.23V vs. RHE. As the  $P_{O_2}$  was increased, the samples became photoactive and the photocurrent density kept increasing up to a maximum reached at a  $P_{O_2}$  of  $1.9 \times 10^{-4}$  mbar. Beyond  $1.9 \times 10^{-4}$  mbar, the photocurrent density progressively decreased to negligible values.

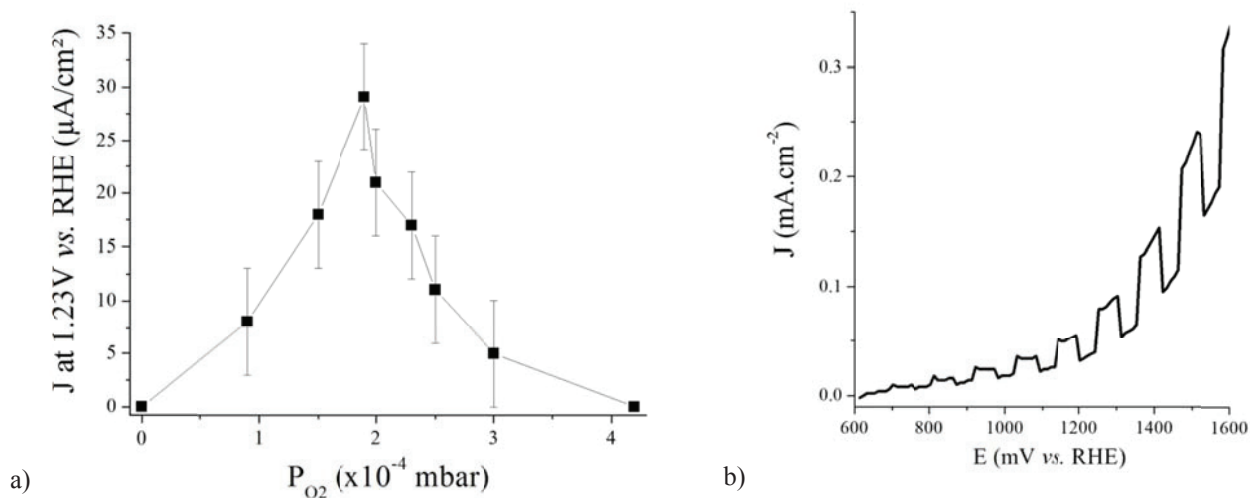


Figure 4: a) Photocurrent densities ( $J$ ) measured at a potential of 1.23 V vs. RHE as a function of the  $P_{\text{O}_2}$  and b) current density-voltage curve of a  $\text{TaO}_x\text{N}_y$  photoanode deposited with a  $P_{\text{O}_2}$  of  $1.9 \times 10^{-4}$  mbar. The PEC measurements were performed in a 0.1M of  $\text{Na}_2\text{SO}_4$  aqueous electrolyte under a AM1.5 irradiation.

The existence of such a photocurrent maximum might be the result of a trade-off between the photoelectrodes' chemical composition, their stability, their morphology, their absorption properties as well as their crystallinity.

First, the increase of the  $P_{\text{O}_2}$  led to the increase of the oxygen content. According to Nakamura *et al.*: (i) metal-N bonds are weaker than metal-O bonds in  $\text{MO}_x\text{N}_y$  compounds which raises stability issues as the N content is increased; (ii) the photooxidation on TaON could be mediated by a nucleophilic attack of water molecules on surface holes which would result in the oxidation of the TaON surface and therefore, in the formation of a thin Ta-oxide overlayer. Thus the more nitrated the  $\text{TaO}_x\text{N}_y$  films are, the more oxidation could occur at the  $\text{TaO}_x\text{N}_y$  films' surface which might exacerbate stability issues; (iii) as the nitrogen content is increased in  $\text{MO}_x\text{N}_y$  compounds, photogenerated holes are trapped at higher levels at the surface, which can decrease the oxidation power of holes [12]. Thus, the initial improvement of the photocurrent densities observed when the  $P_{\text{O}_2}$  was increased could be the result of better stability and stronger oxidation power of the holes.

Second, the increase of the  $P_{\text{O}_2}$  led to the increase of the films roughness and therefore, to the increase of their surface area. This would increase the number of reactional sites for water oxidation and thus, could also be responsible for the initial improvement of the photocurrent densities.

Third, the increase of the  $P_{\text{O}_2}$  led to an increase of the band gap energy due to the lowering of the valence band position. Thus, the decrease of the photocurrent densities beyond a  $P_{\text{O}_2}$  of  $1.9 \times 10^{-4}$  mbar could be assigned to poorer absorption properties.

Fourth, the increase of the  $P_{\text{O}_2}$  resulted in the amorphization of the deposited layers. As structural imperfections can act as recombination centers for photogenerated holes, the amorphization of the photoelectrodes will lead to the degradation of their performance. Thus, in addition to less optimal absorption properties, the decrease of the photocurrent densities beyond a  $P_{\text{O}_2}$  of  $1.9 \times 10^{-4}$  mbar might also be due to increased charge carrier recombination which overcomes the aforementioned benefits brought by the oxygen addition.

The maximal photocurrent density – measured for films deposited with a  $P_{\text{O}_2}$  of  $1.9 \times 10^{-4}$  mbar – was about  $30 \mu\text{A}/\text{cm}^2$ , with an onset potential located at 700 mV vs. RHE (Figure 4b). Such a performance could be considered as quite poor compared to the best performances reported for  $\text{Ta}_3\text{N}_5$  sputtered films or TaON electrophoretically deposited photoelectrodes [5, 7]. But it has to be pointed that no thermal retreatment, no catalyst or no electron scavenger has been employed. If we compare our photocurrent densities – measured without any catalyst or electron scavenger – to the ones of the  $\text{Ta}_3\text{N}_5$  sputtered films prepared by Yokoyama *et al.* and that have been annealed under ammonia to improve the crystallinity, the performances of our sputtered  $\text{TaO}_x\text{N}_y$  films can now

be considered as a good place to start. Thus further improvement of the performances through crystallization and through the use of catalysts could allow us to reach reasonable performances.

#### 4. Conclusion

TaO<sub>x</sub>N<sub>y</sub> photoelectrodes were prepared by DC reactive sputtering at room temperature. The effects of the atmosphere's composition during deposition – *i.e.* a mixture of Ar, N<sub>2</sub> and O<sub>2</sub> – have been investigated. It has been shown that the increase of the P<sub>O<sub>2</sub></sub> led to the amorphization of the films – initially crystallized in the Ta<sub>3</sub>N<sub>5</sub> structural type – as well as to the increases of the films roughness, of their oxygen content and of their bandgap energy. With regard to the photocurrent densities, an optimal P<sub>O<sub>2</sub></sub> has been highlighted. This could correspond to a composition which provided the optimal tradeoff between, on the one hand, the delay of the crystallization and the increase of the bandgap energy – which are usually detrimental for PEC performance – and, on the other, the increases of the films stability and surface area, which are beneficial for PEC performance.

Although the best PEC performances were still pretty low comparing to the one reported in the literature, it is expected that further crystallization and the use of catalysts could allow us to reach reasonable performances in the future. Moreover, the synthesis of such dense films and the precise control of the photoelectrodes characteristics, such as the thickness, the composition and so on, will allow these electrodes to be used for further fundamentals studies. Finally, the use of FTO as substrates is also an advantage since this makes this photoelectrodes suitable for tandem cell devices [13].

#### Acknowledgement

Financial support by the European commission (Project NanoPEC, contract number 227179) is gratefully acknowledged.

#### References

- [1] M. Gratzel, Photoelectrochemical cells, *Nature*, 414 (2001) 338-344.
- [2] F. Tessier, R. Marchand, Ternary and higher order rare-earth nitride materials: synthesis and characterization of ionic-covalent oxynitride powders, *Journal of Solid State Chemistry*, 171 143-151.
- [3] M. Lerch, J. Janek, K.D. Becker, S. Berendts, H. Boysen, T. Bredow, R. Dronskowski, S.G. Ebbinghaus, M. Kilo, M.W. Lumey, M. Martin, C. Reimann, E. Schweda, I. Valov, H.D. Wiemhöfer, Oxide nitrides: From oxides to solids with mobile nitrogen ions, *Progress in Solid State Chemistry*, 37 (2009) 81-131.
- [4] W.-J. Chun, A. Ishikawa, H. Fujisawa, T. Takata, J.N. Kondo, M. Hara, M. Kawai, Y. Matsumoto, K. Domen, Conduction and Valence Band Positions of Ta<sub>2</sub>O<sub>5</sub>, TaON, and Ta<sub>3</sub>N<sub>5</sub> by UPS and Electrochemical Methods, *ChemInform*, 34 (2003) 1798-1803.
- [5] R. Abe, M. Higashi, K. Domen, Facile Fabrication of an Efficient Oxynitride TaON Photoanode for Overall Water Splitting into H<sub>2</sub> and O<sub>2</sub> under Visible Light Irradiation, *J Am Chem Soc*, 132 (2010) 11828-11829.
- [6] A. Ishikawa, T. Takata, J.N. Kondo, M. Hara, K. Domen, Electrochemical Behavior of Thin Ta<sub>3</sub>N<sub>5</sub> Semiconductor Film, *The Journal of Physical Chemistry B*, 108 (2004) 11049-11053.
- [7] D. Yokoyama, H. Hashiguchi, K. Maeda, T. Minegishi, T. Takata, R. Abe, J. Kubota, K. Domen, Ta<sub>3</sub>N<sub>5</sub> photoanodes for water splitting prepared by sputtering, *Thin Solid Films*, 519 (2011) 2087-2092.
- [8] M. Stavrev, D. Fischer, C. Wenzel, K. Drescher, N. Mattern, Crystallographic and morphological characterization of reactively sputtered Ta, TaN and TaNO thin films, *Thin Solid Films*, 307 (1997) 79-88.
- [9] S. Venkataraj, D. Severin, S.H. Mohamed, J. Ngaruiya, O. Kappertz, M. Wuttig, Towards understanding the superior properties of transition metal oxynitrides prepared by reactive DC magnetron sputtering, *Thin Solid Films*, 502 (2006) 228-234.
- [10] Y. Ye, R. Lim, J.M. White, High mobility amorphous zinc oxynitride semiconductor material for thin film transistors, *Journal of Applied Physics*, 106 (2009) 074512-074512-074518.
- [11] O. Banakh, T. Heulin, P.E. Schmid, H. Le Dreo, I. Tkalec, F. Levy, P.A. Steinmann, Influence of process parameters on the properties of the tantalum oxynitride thin films deposited by pulsing reactive gas sputtering, *Journal of Vacuum Science & Technology A: Vacuum, Surfaces, and Films*, 24 (2006) 328-333.

- [12] R. Nakamura, T. Tanaka, Y. Nakato, Oxygen Photoevolution on a Tantalum Oxynitride Photocatalyst under Visible-Light Irradiation: How Does Water Photooxidation Proceed on a Metal–Oxynitride Surface?, *The Journal of Physical Chemistry B*, 109 (2005) 8920-8927.
- [13] J. Brillet, M. Cornuz, F. Le Formal, J.H. Yum, M. Gratzel, K. Sivula, Examining architectures of photoanode-photovoltaic tandem cells for solar water splitting, *Journal of Materials Research*, 25 (2010) 17-24.